



# City Research Online

## City, University of London Institutional Repository

---

**Citation:** Reyes-Aldasoro, C. C. (2009). Retrospective shading correction algorithm based on signal envelope estimation. *Electronics Letters*, 45(9), pp. 454-456. doi: 10.1049/el.2009.0320

This is the unspecified version of the paper.

This version of the publication may differ from the final published version.

---

**Permanent repository link:** <https://openaccess.city.ac.uk/id/eprint/3741/>

**Link to published version:** <https://doi.org/10.1049/el.2009.0320>

**Copyright:** City Research Online aims to make research outputs of City, University of London available to a wider audience. Copyright and Moral Rights remain with the author(s) and/or copyright holders. URLs from City Research Online may be freely distributed and linked to.

**Reuse:** Copies of full items can be used for personal research or study, educational, or not-for-profit purposes without prior permission or charge. Provided that the authors, title and full bibliographic details are credited, a hyperlink and/or URL is given for the original metadata page and the content is not changed in any way.

---

---



# A retrospective shading correction algorithm based on signal envelope estimation

Constantino Carlos Reyes-Aldasoro

Cancer Research UK Tumour Microcirculation Group, Academic Unit of  
Surgical Oncology. The University of Sheffield, K Floor, School of Medicine &  
Biomedical Sciences, Beech Hill Road, Sheffield S10 2RX, U.K.

c.reyes@sheffield.ac.uk

## *Abstract*

An additive retrospective non-parametric algorithm for the correction of inhomogeneous intensity background of images, commonly known as shading, is presented. The algorithm assumed that an original unbiased image was corrupted by a slowly-varying shading that could be estimated from the signal envelope in a process analogous to amplitude modulation detection. Unlike other filtering algorithms, the algorithm did not require pre-processing, parameter setting, user interaction, computationally intensive optimisation algorithms nor a restriction in size of the objects of interest relative to the scale of background variations. The algorithm provided satisfactory results for artificial and microscopical images.

## *Introduction*

A common phenomenon in biomedical imaging is the presence of spurious intensity variations due to the sample of interest and the technique of acquisition. In light microscopy, the variation may originate from uneven sample thickness, out-of-focus objects (in thick slices), or departure from

Köhler illumination and is commonly known as *shading* [1-4]. In magnetic resonance imaging, *intensity inhomogeneity* or *bias field* may be caused by variation in the radio-frequency (RF) coil uniformity, static field inhomogeneity, RF penetration, as well as the anatomy and position of the sample [5-7].

Correction methods can be *prospective* when a calibration protocol and extra images are acquired, or *retrospective* when the only data available is the image itself. When shading is caused by the object, it can only be removed by a retrospective algorithm [8].

The first class of correction algorithms apply *filtering* with low pass, homomorphic or morphological operators as it is a simple and intuitive way of removing low frequency shading components [3]. However, a limitation of these methods is that they assume that the background is either darker or brighter than the objects of interest, and that these are limited in size and smaller than the background variations. In [8] several methods were compared and all filtering methods failed to correct images with large objects.

A second class of algorithms use *surface fitting* methods [3, 9] require the selection of a number of points on the background, either manually or automatically, and the background is obtained by the fitting of a parametric surface. Manual selection is subjective and time consuming and automated methods assume a good global support of the background, which is not always the case. These methods also failed to correct images with large objects. A third class of algorithms perform *entropy minimisation* [4, 10] as it is assumed that the shading introduces extra information to the image, which manifests itself as a higher entropy. A parametric polynomial surface that minimises the entropy is assumed to be the shading component. This method

performed well with all types of images, with either large or small objects. A disadvantage of this method is that an accurate approximation of certain surfaces (one with a small local variation, for example) may require a high order polynomial, and consequently a computationally expensive optimisation process. In practice, the polynomials are restricted to be of lower orders: first or second.

This letter presents an algorithm to remove the shading component of images by estimating the *envelope* of the signal. The process of estimation could be understood as the iterative stretching of a thin flexible surface under which (or over which) a series of objects are placed. Initially, the surface was identical to the signal intensity but after a series of stretches, the surface adapted to the peaks (or lowest points) of the objects, and intermediate values in between them. The algorithm made no assumptions regarding whether the objects were of higher or lower intensity than the background and performed well with small and large objects as well as different microscopical images.

### *Algorithm*

The acquired, shaded image  $I(x,y)$  was assumed to be formed by an additive shading component  $S(x,y)$  which corrupted an original unbiased image  $U(x,y)$

$$I(x,y) = U(x,y) + S(x,y) \quad (1)$$

Therefore, the corrected image  $\hat{U}(x,y)$ , which was an estimation of  $U(x,y)$ , was given by:

$$U(x,y) \approx \hat{U}(x,y) = I(x,y) - S(x,y) \quad (2)$$

The shading correction algorithm estimated the slowly-varying shading component or inhomogeneous background from the envelope of the rapidly-varying signal in a way analogous to the well-known amplitude modulation (AM) detection where a slowly varying function or modulating signal alters the amplitude (or intensity) of a rapidly varying signal or carrier [11]. First, the signal was low-pass filtered with a  $3 \times 3$  Gaussian kernel to minimise the effects of noise. Then, to obtain the envelope, the algorithm scanned every pixel of the image and compared its intensity with the average value of increasingly distant pairs of opposite 8-connectivity neighbours in 4 orientations:  $[0^\circ, 45^\circ, 90^\circ, 135^\circ]$ . Two series of new surfaces  $S_{\max} / S_{\min}$  were generated by replacing the intensity of the pixel by the maximum/minimum value of the comparison at every distance  $d_i$  for each iteration  $i$ . To obtain the upper envelope  $S_{\max}$ , the intensity of the pixel was replaced with the maximum value of the averages and the pixel itself:

$$S_{\max}^i(x,y) = \max \left\{ \frac{I(x-d_i, y-d_i) + I(x+d_i, y+d_i)}{2}, \frac{I(x+d_i, y-d_i) + I(x-d_i, y+d_i)}{2}, \right. \\ \left. \frac{I(x-d_i, y) + I(x+d_i, y)}{2}, \frac{I(x, y-d_i) + I(x, y+d_i)}{2}, I(x,y) \right\} \quad (3)$$


---

For the lower envelope, the replacement corresponded to the minimum value. The maximum/minimum values of the series of surfaces formed two stacks from which the maximum intensity projection corresponded to the current envelope estimation:  $S_{\min}^i(x,y) = \min_i \{S_{\max}^i(x,y)\}$ . Both surfaces  $S_{\max}^i / S_{\min}^i$  were smoothed with a Gaussian low pass filter of size proportional to the distance  $d_i$

to spread the envelope estimation to those pixels with intermediate orientations. The process was repeated by increasing  $d_i$  and the size of the filter, thus allowing the envelope to adapt to objects of different sizes. To determine a stop criterion, local derivatives

---


$$\frac{\partial S_{\max/\min}^i}{\partial x}, \frac{\partial S_{\max/\min}^i}{\partial y}, \quad (4)$$

and the magnitude of the gradient ( $MG^i$ ) were calculated:

$$MG^i = \left( \left( \frac{\partial S_{\max/\min}^i}{\partial x} \right)^2 + \left( \frac{\partial S_{\max/\min}^i}{\partial y} \right)^2 \right)^{\frac{1}{2}}, \quad MG_{tot}^i = \sum_{x,y} MG^i. \quad (5)$$

At every iteration of  $d_i$ ,  $MG_{tot}^i$  was compared with the previous gradient  $MG_{tot}^{i-1}$ ,

and when  $\frac{MG_{tot}^i - MG_{tot}^{i-1}}{MG_{tot}^{i-1}} < 0.01$  the iterations stopped. Finally, the smoothest

surface, either  $S_{\max}^i$  or  $S_{\min}^i$  whichever had a lower  $MG_{tot}^i$ , was assigned as the shading  $S$ .

## Results

The algorithm was tested on images with different characteristics: a histological section stained by immunohistochemistry (Fig. 1a), the vasculature of a tumour from intravital observation (Fig. 1b) and two artificial images (Fig. 1c,d) with objects of different sizes. While the cells of Fig. 1a present objects of interest of a relatively small size, the vessels of Fig. 1b have a larger size and even larger are the chequered squares of Fig. 1c and the irregular shapes of Fig. 1d. The objects of interest in Fig. 1d are of similar size and nature as the image that most algorithms failed to correct in [8]. The central column presents the surfaces that corresponded to the shading of the

images. It should be noted how these surfaces, although slowly varying, would require a high order polynomial for an accurate approximation. The right column shows the corrected images. It is noticeable that all the images now have uniform levels. A profile of each image is presented in Fig. 2. The left column shows the original shaded image (black line) together with the envelope (grey discontinuous line). While for Fig. 2a,c the shading corresponded to  $S_{\max}^i$ , for Fig. 2b,d the shading corresponded to  $S_{\min}^i$ . In other words, the background in the first case was considered as bright (high intensity) while on the second case it was considered dark (low intensity). It is also important to notice that in the four cases, the shading was corrected as all the profiles on the right column show uniform intensity levels regardless of the size of the objects that increase in size from top to bottom.

As an indication of the computational complexity, 28 iterations were required to process a  $342 \times 342$  image (Fig. 1c) and the average time was 5.4 s (Matlab version 7.4.0.287 (R2007a) running on a Mac PowerBook 2.6 GHz Intel Core 2 Duo, 4 GB RAM, OS X 10.5.5). As a comparison, entropy optimisation with the *fminsearch* Matlab algorithm of the 10-parameter second order polynomial proposed in [4] took 45.6 s.

### *Conclusion*

An algorithm based on the envelope detection of image intensities was presented. The algorithm corrected the shading of different types of images and did not require the objects of interest to be small in size nor the use of computationally expensive optimisation algorithms. The spurious intensity variations were corrected even when the surfaces would not be easily described by a low-order polynomial function. The algorithm could be a pre-

processing step for segmentation or quantitative analysis and only requires user intervention to confirm accuracy. This algorithm can be widely used in biomedical imaging, from microscopy to magnetic resonance.

### *Acknowledgements*

This work was funded by Cancer Research UK.

### *References*

- [1] S. Inoué, *Video Microscopy*. New York: Plenum Press, 1986.
- [2] A. L. D. Beckers, W. C. Debruijn, E. S. Gelsema, M. I. Cleton-Soeteman, and H. G. Vaneijk, "Quantitative Electron Spectroscopic Imaging in Bio-Medicine - Methods for Image Acquisition, Correction and Analysis," *J Microsc*, vol. 174, pp. 171-182, 1994.
- [3] J. C. Russ, *The Image Processing Handbook*, 2nd ed. Boca Raton, FL: IEEE Press, 1995.
- [4] B. Likar, J. B. A. Maintz, M. A. Viergever, and F. Pernus, "Retrospective shading correction based on entropy minimization," *J Microsc*, vol. 197, pp. 285-295, 2000.
- [5] A. Simmons, P. S. Tofts, G. J. Barker, and S. R. Arridge, "Sources of Intensity Nonuniformity in Spin-Echo Images at 1.5-T," *Magnetic Resonance in Medicine*, vol. 32, pp. 121-128, 1994.
- [6] B. Likar, M. A. Viergever, and F. Pernus, "Retrospective correction of MR intensity inhomogeneity by information minimization," *IEEE Trans Med Imaging*, vol. 20, pp. 1398-1410, 2001.
- [7] B. R. Condon, J. Patterson, D. Wyper, P. a. Jenkins, and D. M. Hadley, "Image Nonuniformity in Magnetic-Resonance-Imaging - Its Magnitude and Methods for Its Correction," *BJ Radiol*, vol. 60, pp. 83-87, 1987.
- [8] D. Tomazevic, B. Likar, and F. Pernus, "Comparative evaluation of retrospective shading correction methods," *J Microsc*, vol. 208, pp. 212-223, 2002.
- [9] Z. J. Hou, S. Huang, Q. M. Hu, and W. L. Nowinski, "A fast and automatic method to correct intensity inhomogeneity in MR brain images," *Medical Image Computing and Computer-Assisted Intervention - MICCAI 2006, Pt 2*, vol. 4191, pp. 324-331, 2006.
- [10] U. Vovk, F. Pernus, and B. Likar, "Intensity inhomogeneity correction of multispectral MR images," *Neuroimage*, vol. 32, pp. 54-61, 2006.
- [11] B. P. Lathi, *Modern Digital and Analog Communication Systems*, 3rd ed. Oxford: Oxford University Press, 1998.

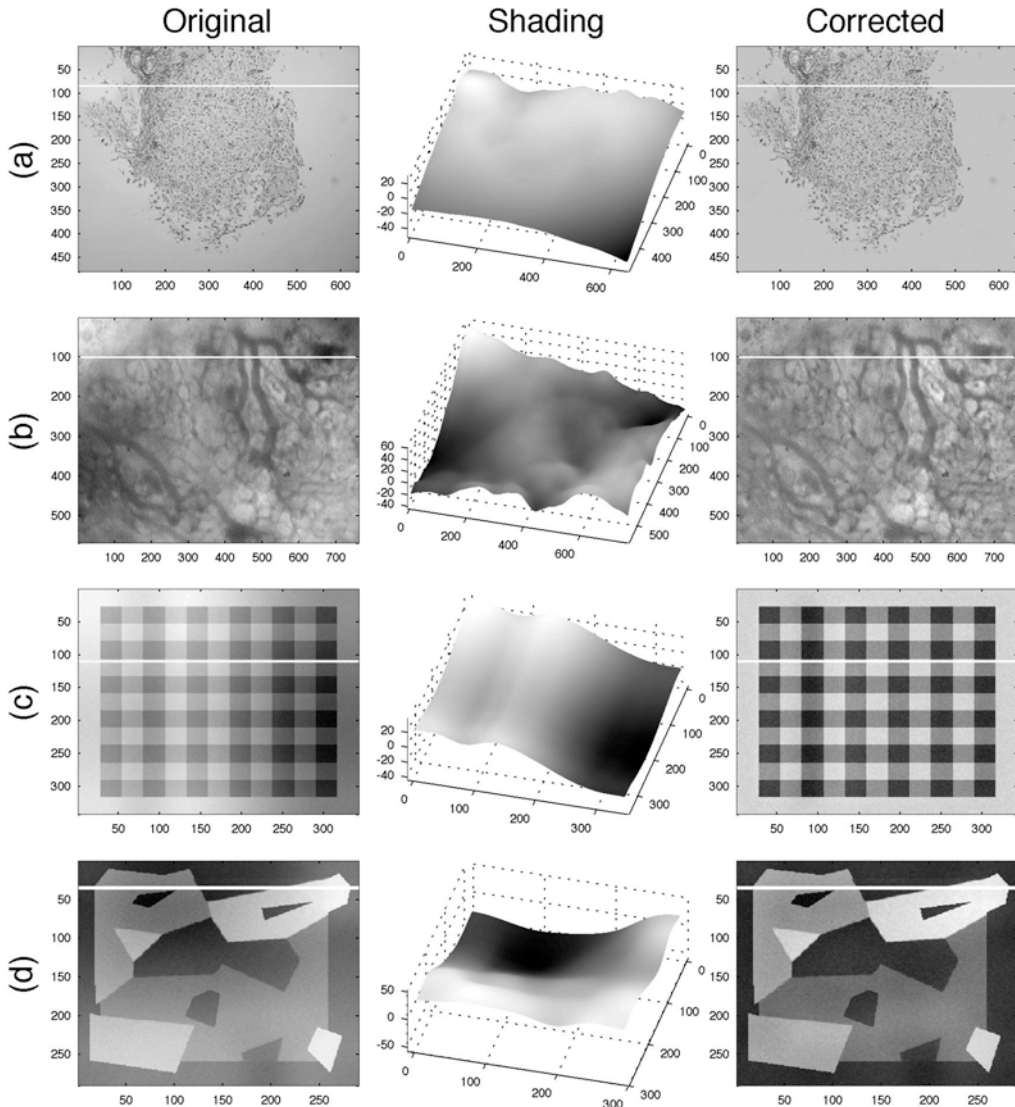


Fig. 1. Left column: four representative images with associated shading: (a) a histological tissue section stained with immunohistochemistry, (b) an intravital microscopical image of the vasculature of a tumour, (c) chequered test pattern, (d) test image with large irregular objects. Images (c,d) were corrupted with a bias field and Gaussian noise. Central column: the additive shading component of the images shown as a 3D surface. It is important to notice that the shading would not be easily described by a polynomial function. Right column: intensity corrected images. The white lines correspond to the profiles shown in Fig. 2.

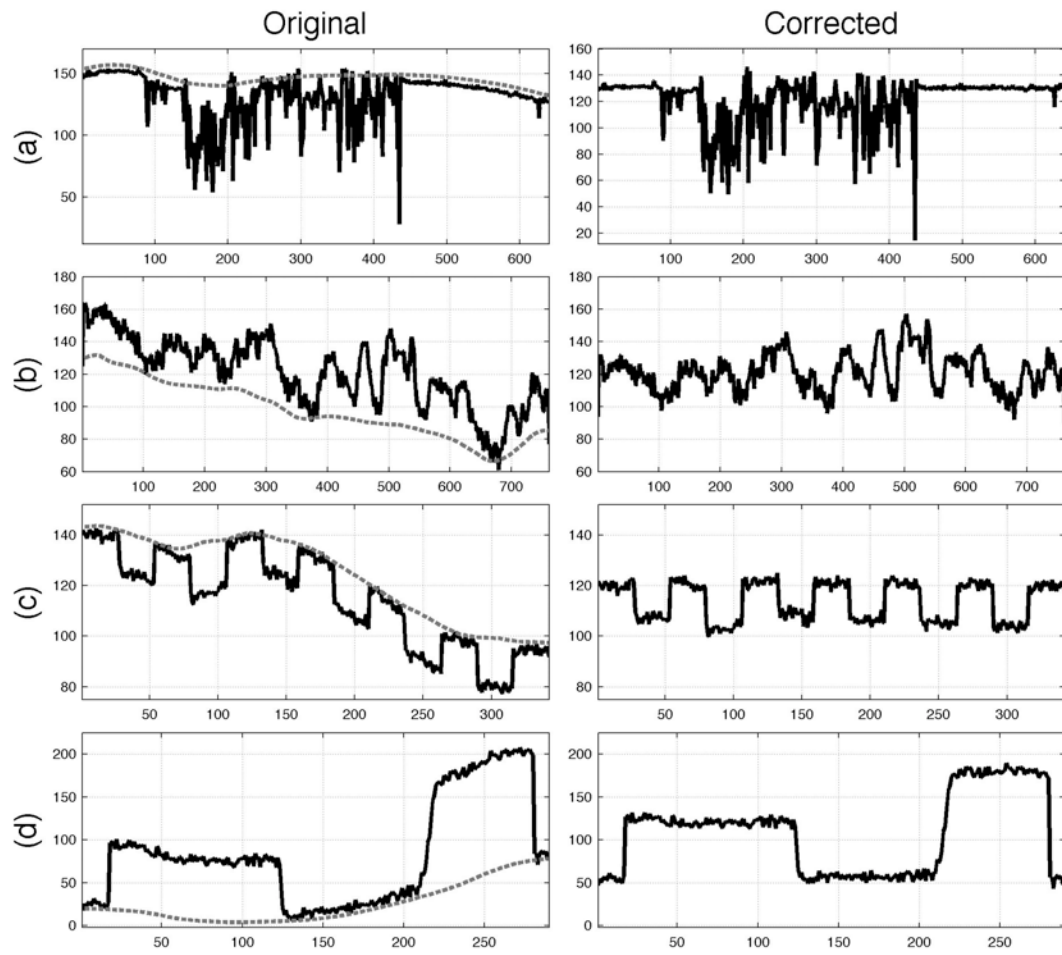


Fig. 2 Left column: intensity profiles of the original images, (a) immunohistochemistry, (b) intravital microscopy, (c,d) test images. Black solid line corresponds to the image, and a dashed grey line to the estimated envelope. In (a, c) the envelope was assumed as a maximum while for (b,d) it was a minimum. Right column shows the corrected profiles.